

1 **Expanding the clinical tumor phenotype of the EPAS1-associated tumor syndrome**

2 **Authors:** Yasemin Cole¹(Orchid ID 0000-0002-9492-5885), Sophie Howarth², Asna Javaid³, Patrick
3 Tarpey³, Daniel Scoffings⁴, Eamonn R Maher^{1,5}, Anna L Godfrey⁶, Karel Pacak^{7,8,9}, Zhengping
4 Zhuang¹⁰, Hussam Alkaissi¹¹, Ruth T Casey (Orchid ID 0000-0003-4058-3135)^{1,2}

5
6 **Affiliations:** ¹Department of Genomic Medicine, University of Cambridge, Cambridge Biomedical
7 Campus, Cambridge, UK; ²Department of Endocrinology, Cambridge University Hospital,
8 Cambridge Biomedical Research Centre, Addenbrooke's Hospital, Cambridge, UK; ³Molecular
9 Genetic Laboratories, Cambridge University Hospital, Cambridge Biomedical Research Centre,
10 Addenbrooke's Hospital, Cambridge, UK; ⁴Department of Radiology, Cambridge University
11 Hospital, Cambridge Biomedical Research Centre, Addenbrooke's Hospital, Cambridge, UK; ⁵Aston
12 Medical School, College of Health and Life Sciences, Birmingham, UK; ⁶Department of
13 Haematology, Cambridge University Hospitals, NHS Foundation Trust, Cambridge, UK; ⁷Section on
14 Medical Neuroendocrinology, *Eunice Kennedy Shriver* National Institute of Child Health and Human
15 Development, National Institutes of Health, Bethesda, MD 20892, USA; ⁸Center for Adrenal
16 Endocrine Tumors, AKESO, Prague 5, Czech Republic 158 00; ⁹Multidisciplinary Consortium for
17 Adrenal Diseases, Faculty of Medicine and Faculty Hospital, Palacky University, Olomouc, Czech
18 Republic; ¹⁰Neuro-Oncology Branch, National Cancer Institute, National Institutes of Health,
19 Bethesda, MD 20892, United States; ¹¹National Institute of Diabetes and Digestive and Kidney
20 Diseases, National Institutes of Health, Bethesda, MD 20892, USA

21

22

23

Key Words:

EPAS1, pancreatic neuroendocrine tumor, paraganglioma/pheochromocytoma, genotype-phenotype

To whom correspondence should be addressed: Ruth Casey, MD, PhD, Consultant Endocrinologist, Department of Endocrinology, Cambridge University Hospital, Cambridge Biomedical Research Centre, Addenbrooke's Hospital, Cambridge, UK CB2 0QQ. Email: rc674@medschl.cam.ac.uk

8
9 Funding: This research was in part supported by the Intramural Research Programs of the National
10 Institute of Diabetes and Digestive and Kidney Diseases (NIDDK), the *Eunice Kennedy Shriver*
11 National Institute of Child Health and Human Development (NICHD), the National Cancer Institute
12 (NCI), the National Institute of Neurological Disorders and Stroke (NINDS), and the National Heart,
13 Lung, and Blood Institute (NHLBI), within the National Institutes of Health (NIH). The contributions
14 of the NIH author(s) are considered Works of the United States Government. The findings and
15 conclusions presented in this paper are those of the author(s) and do not necessarily reflect the
16 views of the NIH or the U.S. Department of Health and Human Services. Additionally, it was in part
17 funded by the Paradifference Foundation. Ruth Casey and Eamonn Maher receive funding from
18 NIHR Cambridge Biomedical Research Centre (NIHR203312). The views expressed are those of the
19 authors and not necessarily those of the NIHR or the Department of Health and Social Care.
20 Yasemin Cole receives funding from the NIH Oxford-Cambridge Scholars Program and Gates
21 Cambridge Scholars Program.

1 Conflict of Interest Disclosure: The authors have nothing to declare.

2

3 **Abstract**

4 *Context:* Since the original discovery of the Pacak-Zhuang syndrome (PZS) in 2012, defined
5 by the clinical triad of pheochromocytoma/paraganglioma (PPGL) and/or duodenal
6 ampullar somatostatinoma with erythrocytosis, multiple multisystemic phenotypes have
7 been identified in patients with somatic mosaic pathogenic variants in *EPAS1/HIF2A*. Deep
8 phenotyping of patients along with evaluation of a transgenic murine model has led to the
9 understanding of the role of HIF-2 α in developmental processes, including tumor
10 development. Interestingly, pancreatic NETs occur in von Hippel-Lindau disease and the
11 *VHL* gene product regulates HIF-2 α expression.

12 *Objective and results:* Herein, we describe a novel series from two institutions of patients
13 with *EPAS1* associated pancreatic neuroendocrine tumors including a case of a
14 nonfunctioning pancreatic neuroendocrine tumor (NET) in association with an *EPAS1*
15 somatic mosaic variant. This case study extends our current understanding of the
16 phenotypic spectrum in PZS and links pancreatic NETs to an additional hypoxia-associated
17 gene, namely *EPAS1*.

18

19 **Introduction**

20 In the early 2000s, members of a family with erythrocytosis were found to have a novel
21 germline *EPAS1/HIF2A* gain-of-function variant[1]. At the same time, patients with VHL-

1 associated Chuvash erythrocytosis (homozygous *VHL* c.598C>T variants) uniquely present
2 with blood cell dyscrasias and elevated vascular endothelial growth factor (VEGF) in the
3 absence of tumors[2]. Taken together, this led to the concept that HIF-2 α (encoded by
4 *EPAS1/HIF2A*) may be involved in erythrocytosis. Mosaic postzygotic gain-of-function
5 variants in *EPAS1/HIF2A* were then identified in two individuals with congenital
6 erythrocytosis, pheochromocytoma/paraganglioma (PPGL), and duodenal ampullar
7 somatostatinoma, connecting for the first time, *EPAS1* to tumor development[3, 4].

8

9 Concurrent to the discovery of this syndrome, a transgenic murine model bearing a mosaic
10 variant, introduced early in embryonic development, solidified our understanding of the
11 role of *EPAS1* in PPGL development[5]. This model reproduced the clinical spectrum of
12 Pacak-Zhuang syndrome (PZS) including erythrocytosis and somatostatinoma positive
13 cells within the duodenal ampulla. Deep phenotyping and assessment of patients with PZS
14 with the PPGL clinical program at the National Institutes of Health[6, 7] have revealed that
15 patients and mice have unexpected multisystemic malformations, likely a reflection of the
16 spatiotemporal expression of HIF-2 α during embryonic development[8]. Beyond
17 erythrocytosis and neural crest derived PPGL tumors, *EPAS1* gain-of-function variants have
18 been linked to ocular defects (e.g., tortuous retinal vessels, optic nerve gliosis, morning
19 glory anomalies, retinal and macular edema), systemic venule malformations (e.g.,
20 cavernous malformations in the spinal vascular network), enlarged venous drainage of the
21 central nervous system (vein of Galen and dural sinuses), and neural tube defects (e.g.,

1 neuraxial dysraphism) within patients and the corresponding transgenic mouse model
2 (Figure 1)[9-11].

3

4 Pancreatic neuroendocrine tumors (NETs) are a feature of some inherited cancer
5 syndromes, including multiple endocrine neoplasia type 1 (MEN1), von-Hippel Lindau
6 (VHL) disease and, occasionally, in patients with germline pathogenic variants in succinate
7 dehydrogenase subunit B and subunit D gene (*SDHB* and *SDHD*, respectively) and
8 neurofibromatosis (*NF1*)[12, 13]. Extensive whole exome and genome sequencing studies
9 have revealed that a sizeable percentage of pancreatic NETs are heritable (17%) and can
10 harbor germline and somatic pathogenic variants in *VHL*, *NF1*, and *ATRX*, similar to PPGLs,
11 and genetic defects impacting the PI3K/mTOR pathway (e.g., *TSC1/2*, *PTEN*)[14-16]. Scarpa
12 et al. identified a distinct cluster of pancreatic NETs associated with hypoxia signaling and
13 metabolic reprogramming[14]. More recent work by Yossef et al., investigating
14 metabolomics and transcriptomics profile of pancreatic NETs in VHL vs non-VHL patients,
15 showed a unique profile of pseudohypoxic NETs, with abundance of adenosine and its
16 metabolites in pseudohypoxic tumors[17]. The penetrance of pancreatic NETs in *VHL*
17 carriers ranges between 8-17% and tumors are typically non-functioning but may be
18 malignant[18]. The *VHL* locus is often inactivated in sporadic pancreatic NETs through non-
19 mutational mechanisms and is associated with reduced survival rates[19]. Both sporadic
20 and hereditary pancreatic NETs with *VHL* inactivation are associated with upregulated HIF-
21 2α activity and the expression of hypoxia responsive genes. To date, molecular drivers of
22 PNETs have not been linked to *EPAS1*.

1
2 The vast majority of genetic variants in *EPAS1* are somatic mosaic and/or occur in the
3 oxygen dependent degradation (ODD) domain (residues 529 to 540), however variants 3' of
4 the ODD have been identified impacting residues 766, 785-789, and 834 [6, 20-23]. Recent
5 studies have suggested the role of environmental hypoxia exposure (e.g., sickle cell
6 disease, congenital cyanotic heart disease, and altitude) driving acquired somatic *EPAS1*
7 variants in PPGLs and epigenetic modulation of *EPAS1* as an adaptation response, however
8 it is unclear whether they are inciting factors[24-27]. In addition, it is uncertain whether
9 chronic hypoxia increases the risk for other tumors. Thus far, none of the reported studies
10 of patients with somatic mosaic PZS and those with environmental hypoxia exposure have
11 reported pancreatic NETs, except for somatostatinoma(s)[28]. There have been reports of a
12 somatic *EPAS1* variant in a pancreatic neuroendocrine tumor (NET) (p.Pro531His) and
13 germline *EPAS1* variant in individual with concomitant VHL syndrome and an additional
14 case of a pancreatic NET (with germline variants in *VHL* Trp117Ser and *EPAS1* p.
15 His194Arg)[20, 29].
16
17 Belzutifan, a potent HIF-2 α inhibitor (PT2977), was first evaluated in VHL-associated renal
18 cell carcinoma and showed therapeutic benefit with objective response rates of 49%[30]. It
19 has likewise proven to be effective in other VHL disease cancer phenotypes with a 91%
20 therapeutic response rate in patients with pancreatic NETs[30, 31], suggesting a role of
21 Belzutifan in treating *EPAS1*-associated pancreatic NETs. Recent studies indicate that

1 Belzutifan has activity in all clear cell renal carcinoma with an objective response rate of
2 21.9-25% at a median follow up of >25 months[32, 33]. In addition, Belzutifan has been
3 used in cases of PZS with therapeutic effects on hemoglobin, erythropoietin,
4 catecholamines, blood pressure control, and tumor control[34-36] along with advanced or
5 metastatic pheochromocytomas and paragangliomas[37]. Belzutifan has recently gained
6 FDA approval for usage in clear cell renal carcinoma as well as pheochromocytoma and
7 paraganglioma in the United States. Herein, we describe a novel case of pancreatic NET, in
8 the absence of synchronous PPGLs in an individual with PZS and investigate the phenotype
9 of pancreatic NETs in a case series of patients with somatic mosaic pathogenic variants in
10 *EPAS1*.

11

12 **Materials and Methods**

13 *Study Design and Patient Selection*

14 All patients included in the study provided written informed consent in accordance with the
15 ethical standards established by the Helsinki Declaration. The index patient was recruited
16 to the Molecular Pathology of Human Genetic Disease Study (South Birmingham REC
17 CA/125) at Addenbrooke's Hospital. Likewise, the institutional review board of the *Eunice*
18 *Kennedy Shriver* National Institute of Child Health and Development (NICHD,
19 ClinicalTrials.gov Identifier: NCT00004847) approved the pheochromocytoma
20 paraganglioma clinical study protocol. Patients with paraganglioma(s), erythrocytosis, and
21 confirmed *EPAS1* somatic mosaic variant in the NICHD study met the criteria of PZS.

1 *Cohort Evaluation and Genetic Analysis*

2 The pathogenic *EPAS1* variant (Asp539His) in the index case was first identified on NHS
3 clinical sequencing endocrine neoplasia and hereditary erythrocytosis panels by next
4 generation sequencing. Subsequently, the variant allele frequency in both the pancreatic
5 NET and blood of the index patient were evaluated using custom designed Sanger
6 sequencing primers targeting the ODD of *EPAS1*. For PZS patients at the NIH, variants in the
7 *EPAS1* ODD were evaluated in circulating leukocytes and/or resected tumors utilizing
8 whole exome sequencing, ddPCR, peptide nucleic acid sequencing and were previously
9 shown to be somatic mosaic in patient tissue[6, 9, 38]. Phenotypic data along with lab
10 results were collected from respective institutional electronic health records.

11

12 **Results**

13 **Case Presentation**

14 A male infant was referred to the ophthalmology team with concerns regarding severe
15 visual impairment and was registered as blind secondary to bilateral congenital retinal
16 dysplasia at 3 months old. His family history was notable for Factor V Leiden deficiency
17 and a maternal uncle with seizures and intellectual disability of unknown etiology. Genetic
18 testing for Norrie's disease (associated with *NDP* pathogenic variants) and exudative
19 vitreoretinopathy (linked to variants in *FZD4*, *LRP5* and *TSPAN12*) were negative.

20

1 The patient underwent tonsillectomy at age nine which was complicated by two episodes
2 of post-operative hemorrhage. Blood tests showed a persistently elevated hemoglobin of
3 204 g/L (115-155g/L), hematocrit of 0.677 (0.350-0.450 L/L), platelets of 134 x10⁹/L (150-
4 400 x10⁹/L) and prolonged prothrombin time of 14 s (9.8-12.6 s). Blood film showed packed
5 red cells with morphologically normal white cells and platelets, white cell differential was
6 normal, and his blood tests were otherwise unremarkable except for marginally elevated
7 total bilirubin of 16 µmol/L (0-14µmol/L).

8

9 He was referred to the pediatric hematology team who performed extensive investigations
10 for primary and secondary erythrocytosis. PCR testing of JAK2 V617F and JAK2 exon 12
11 pathogenic variants were both negative, hemoglobin electrophoresis was normal, clotting
12 factor assays were normal, but his erythropoietin level was significantly elevated at 614 U/L
13 (5-25 U/L) and iron studies were consistent with iron deficiency. The patient had serial
14 whole-body MRI, ultrasound, echocardiogram and [¹⁸F]-FDG PET-CT imaging over a period
15 of 3 years which was negative for any cardiac congenital abnormality or erythropoietin-
16 secreting source such as a hemangioblastoma, revealing only mild splenomegaly.
17 Differential renal venous sampling was performed but was normal. MRI imaging of the head
18 also demonstrated prominent perivascular spaces in the subcortical white matter of both
19 cerebral hemispheres of unclear clinical significance and bilateral enophthalmos (Figure
20 2). Bone marrow aspirate and trephine revealed a hypercellular marrow with erythroid
21 hyperplasia and no features of dysplasia or increased blasts. The possibility of a

1 pathogenic variant in the oxygen-sensing pathway or high-affinity hemoglobin was
2 discussed, but genetic screens for *VHL*, *PHD2* and *EPAS1* were initially negative.

3

4 In the interim, he was commenced on a program of intermittent venesection. Following a
5 period of suboptimal hematocrit control, CT imaging was repeated for abdominal pain. This
6 showed a new non-occlusive thrombus in the splenic vein in addition to known
7 splenomegaly, features suggestive of non-cirrhotic portal hypertension and a pancreatic
8 lesion. He was started on oral anticoagulation and endoscopic ultrasound was performed
9 showing a 24 mm uncinate process lesion and an adjacent 10 mm lymph node. Fine needle
10 aspirate from both lesions was in keeping with a well differentiated neuroendocrine tumor,
11 showing cells with granular, coarse hyperchromatic chromatin patterns and scant
12 eosinophilic cytoplasm which were positive on immunohistochemical staining for
13 MNF116, synaptophysin, chromogranin A and CD56. MIB -1 proliferation index was <3%.
14 Clinically, the patient reported no symptoms/signs of hormone excess, specifically he had
15 no gastrointestinal symptoms and fasting gut peptide screening revealed a normal
16 somatostatin level. Subsequent staging with a Gallium-68 [⁶⁸Ga]-DOTATATE PET-CT scan
17 demonstrated high somatostatin receptor expression in the pancreatic lesion and adjacent
18 node, with no other evidence of metastatic disease (Figure 2). The working diagnosis was
19 that of a non-functioning pancreatic neuroendocrine tumor and after careful discussion, a
20 Whipple's resection was performed. Histology confirmed a grade 2, well differentiated
21 pancreatic NET, ENETS stage pT2 N1 R0.

1 A liver biopsy was arranged to investigate non-cirrhotic portal hypertension and
2 demonstrated features of portosinusoidal vascular disorder with an overall mild portal and
3 perisinusoidal fibrosis. Esophago-gastroduodenoscopy was negative for any varices. In
4 view of this new diagnosis of a pancreatic NET, genetic testing included an endocrine
5 neoplasia panel (*AIP*, *CDC73*, *CDKN1B*, *MEN1*, *RET* exons 5, 8, 10, 11 and 13-16) and a
6 repeat hereditary erythrocytosis panel (R405) by next generation sequencing was also
7 performed. These analyses were performed using the standardized genetic testing panels
8 commissioned through the NHS. A mosaic likely pathogenic *EPAS1* variant c.1615G>C p.
9 (Asp539His) was identified in germline blood samples taken at age 2 and 22, with a variant
10 allele frequency of 13%.

11

12 Targeted Sanger sequencing also identified the same *EPAS1* variant in the pancreatic NET
13 sample at a variant allele frequency of 42.8% (Figure 2). In addition, targeted Sanger
14 sequencing validated the germline results: the variant allele frequency in the blood
15 samples were 15.2% and 15.5%. Utilizing ACMG criteria for pathogenicity, the Asp539His
16 variant met the criteria for likely pathogenicity with the following lines of evidence: PM1,
17 PM2, PP3, PS3, and PS4. The variant was not identified in gnomAD nor ExAC (PM2) and is
18 located in a hotspot region of the oxygen dependent degradation domain of EPAS1 (PM1).
19 Ferens et al. reported the class 1 Asp539Tyr and Asp538Asn variants impact binding with
20 PHD2, leading to increased transcriptional activity of EPAS1 (PS3). *In silico* prediction
21 models are congruent and predict the variant to be pathogenic (PP3): SIFT 0 (deleterious),
22 Polyphen score 1 (probably damaging), CADD score of 31 (deleterious, top 0.1%), and

1 alpha missense score 0.9977 (likely pathogenic). Somatic sequencing using a commercial
2 gene panel assay via the TruSight Oncology 500 (TSO500) assay, which interrogates over
3 500 cancer-related genes, was performed on DNA extracted from the pancreatic NET and
4 no additional somatic variants were identified. Serial plasma metanephhrines have been
5 normal to date with no evidence of synchronous PPGLs on cross sectional imaging or
6 [⁶⁸Ga]-DOTATATE PET-CT. Serial imaging has not identified recurrence of the pancreatic NET
7 almost two years post-surgery.

8

9 ***Review of pancreatic phenotypes in mosaic EPAS1 (HIF2A) gain-of-function syndrome***
10 ***“Pacak-Zhuang syndrome”***

11 *EPAS1* somatic mosaic variants are a hallmark of neuroendocrine tumors in PZS. In the 15
12 cases at the NIH, five individuals, followed for at least 11 years since first tumor evaluation,
13 developed histologically confirmed pancreatic NET with oftentimes dilation of the
14 pancreatic duct, in addition to PPGL(s) at or after the diagnosis of erythrocytosis (Figure 3).
15 Among those five patients, erythrocytosis was first diagnosed at a median age of 2 years
16 (range: birth to 7 years). The median age at diagnosis of PPGL was 24.4 years (range: 14–39
17 years), while pancreatic NETs (PNETs) were diagnosed at a median age of 29 years (range:
18 21–39 years) and metastatic PNETs occurred in 3 out of 5 cases. The cohort was
19 predominantly female, with a female-to-male ratio of 4:1. The median somatostatin levels
20 was 47.6 pg/mL (normal range up to 25 pg/mL) across the group (range: 12–109 pg/mL),
21 including a patient with normal somatostatin levels, similar to our reported index case,

1 thus a normal somatostatin level does not exclude the diagnosis of NET in patients with
2 PZS. Despite having a pathogenic variant at codon 539, similar to this case study, patient
3 #1 in the NIH cohort had a functional somatostatin-producing PNET and had post-surgical
4 cystic changes (Figure 3). All cases presented symptomatically with non-specific
5 generalized gastrointestinal symptoms/signs and somatostatin secreting PNETs at an older
6 onset (age range 21-39) than this case study and with multiple tumors, local recurrence
7 and distant metastasis in 75%, 75%, and 50%, respectively (Table 1). Resected PNETs had
8 *EPAS1* variants at a variant allele frequency of 31-56% of the tumor content, a similar
9 percentage to our index case (42.8%). Critically, two of the individuals developed
10 recurrence and metastasis and three individuals (Patient #1, #2, and #4) were commenced
11 on Belzutifan after recurrence of PPGL and without surgical resection. To date, Patient #2
12 has had limited disease progression on imaging after 17 months of treatment. Patients #1,
13 #2, and #4 have had stable somatostatin levels since initiating Belzutifan.

14

15 **Discussion**

16 This case study of a non-functioning NET in an individual with congenital erythrocytosis,
17 bilateral cataracts, and splenomegaly is the first reported case of an individual with a non-
18 functioning PNET and pathogenic *EPAS1* variant. This case study describes a new genetic
19 etiology of PNETs. Approximately 10% of individuals with VHL disease, with higher
20 frequencies in those with PPGL predisposing missense variants, develop pancreatic NETs,
21 which are often non-functioning and multifocal [18, 39, 40]. Recently, proteomic

1 assessment and differential gene expression of pancreatic NETs have identified the
2 molecular subtypes metastasis-like (MLP) tumors, associated with a poor prognosis, and
3 are characterized by upregulated hypoxia signaling such as HIF-1 α expression[41], however
4 underlying genetic pathogenic variants in hypoxia signaling pathways beyond *VHL* were not
5 identified. The identification of direct binding of HIF-2 α with β -catenin[42] supports the
6 involvement of downstream HIF-2 α signaling in the pathophysiology of PNETs. Landmark
7 studies of the therapeutic efficacy with the potent small-molecule inhibitor of HIF-2 α
8 Belzutifan in VHL-associated pancreatic lesions in patients with clear cell renal
9 carcinoma[31] suggests that the hypoxia subtype of pancreatic NETs including *EPAS1* may
10 also be amenable to the same therapy and therefore assessment of the frequency of
11 *EPAS1* variants in large cohorts of pancreatic NETs is warranted. However, it should be
12 noted that, as seen with the initial testing in our case, mosaic *EPAS1* variants may not be
13 detected by routine genetic testing and specific molecular investigations may be indicated
14 if low-level mosaic variants are suspected. The efficacy of the HIF-2 α inhibitor Belzutifan
15 has expanded from VHL associated renal tumors to a role in all clear cell renal carcinomas,
16 and metastatic PPG[33] and conceptualizes the larger translational implications of
17 studying rare genetic syndromes and genotype-phenotype correlations. This case series
18 illustrates an expansion of the current understanding of gene-disease phenotypes
19 associated with *EPAS1*, including the association with functioning and non-functioning
20 PNETs. The observation of portosinusoidal vascular liver disease, enophthalmos,
21 prominent perivascular spaces within the brain white matter and a non-functioning
22 pancreatic NET in one individual in this case series supports the possibility of a

1 spatiotemporal effect of the *EPAS1* mosaic variant and warrants further evaluation in a
2 transgenic *EPAS1* murine model.

3

4 **Data Availability**

5 All clinical data were obtained from electronic medical records at Cambridge University
6 Hospitals and the National Institutes of Health. The authors confirm that the data
7 supporting the findings are available within the article. Data sharing is not applicable to this
8 article as no datasets were generated or analyzed during the current study.

9 **References**

- 10 1. Percy MJ, Furlow PW, Lucas GS, Li X, Lappin TR, McMullin MF, et al. A gain-of-
11 function mutation in the HIF2A gene in familial erythrocytosis. *N Engl J Med.* 2008;358(2):162-
12 8.
- 13 2. Gordeuk VR, Sergueeva AI, Miasnikova GY, Okhotin D, Voloshin Y, Choyke PL, et al.
14 Congenital disorder of oxygen sensing: association of the homozygous Chuvash polycythemia
15 VHL mutation with thrombosis and vascular abnormalities but not tumors. *Blood.*
16 2004;103(10):3924-32.
- 17 3. Yang C, Hong CS, Prchal JT, Balint MT, Pacak K, Zhuang Z. Somatic mosaicism of
18 EPAS1 mutations in the syndrome of paraganglioma and somatostatinoma associated with
19 polycythemia. *Hum Genome Var.* 2015;2:15053.
- 20 4. Zhuang Z, Yang C, Lorenzo F, Merino M, Fojo T, Kebebew E, et al. Somatic HIF2A
21 gain-of-function mutations in paraganglioma with polycythemia. *N Engl J Med.*
22 2012;367(10):922-30.
- 23 5. Wang H, Cui J, Yang C, Rosenblum JS, Zhang Q, Song Q, et al. A Transgenic Mouse
24 Model of Pacak(-)Zhuang Syndrome with An Epas1 Gain-of-Function Mutation. *Cancers*
25 (Basel). 2019;11(5).
- 26 6. Darr R, Nambuba J, Del Rivero J, Janssen I, Merino M, Todorovic M, et al. Novel
27 insights into the polycythemia-paraganglioma-somatostatinoma syndrome. *Endocr Relat Cancer.*
28 2016;23(12):899-908.
- 29 7. Rosenblum JS, Wang H, Nazari MA, Zhuang Z, Pacak K. Pacak-Zhuang syndrome: a
30 model providing new insights into tumor syndromes. *Endocr Relat Cancer.* 2023;30(10).
- 31 8. Alkaissi H, Cole Y, Doucet-O'Hare TT, Rosenblum JS, Zhuang Z, Pacak K. A schema
32 for sporadic and heritable disease pathogenesis integrating spatiotemporal distribution with the
33 character of genetic variants. *Commun Med (Lond).* 2025;5(1):340.

1 9. Rosenblum JS, Wang H, Dmitriev PM, Cappadona AJ, Mastorakos P, Xu C, et al.
2 Developmental vascular malformations in EPAS1 gain-of-function syndrome. *JCI Insight*.
3 2021;6(5).

4 10. Rosenblum JS, Cappadona AJ, Argersinger DP, Pang Y, Wang H, Nazari MA, et al.
5 Neuraxial dysraphism in EPAS1-associated syndrome due to improper mesenchymal transition.
6 *Neurol Genet*. 2020;6(3):e414.

7 11. Dmitriev PM, Wang H, Rosenblum JS, Prodanov T, Cui J, Pappo AS, et al. Vascular
8 Changes in the Retina and Choroid of Patients With EPAS1 Gain-of-Function Mutation
9 Syndrome. *JAMA Ophthalmol*. 2020;138(2):148-55.

10 12. Pea A, Hruban RH, Wood LD. Genetics of pancreatic neuroendocrine tumors:
11 implications for the clinic. *Expert Rev Gastroenterol Hepatol*. 2015;9(11):1407-19.

12 13. Niemeijer ND, Papathomas TG, Korpershoek E, de Krijger RR, Oudijk L, Morreau H, et
13 al. Succinate Dehydrogenase (SDH)-Deficient Pancreatic Neuroendocrine Tumor Expands the
14 SDH-Related Tumor Spectrum. *The Journal of clinical endocrinology and metabolism*.
15 2015;100(10):E1386-93.

16 14. Scarpa A, Chang DK, Nones K, Corbo V, Patch AM, Bailey P, et al. Whole-genome
17 landscape of pancreatic neuroendocrine tumours. *Nature*. 2017;543(7643):65-71.

18 15. Backman S, Norlen O, Eriksson B, Skogseid B, Stalberg P, Crona J. Detection of
19 Somatic Mutations in Gastroenteropancreatic Neuroendocrine Tumors Using Targeted Deep
20 Sequencing. *Anticancer Res*. 2017;37(2):705-12.

21 16. Mafficini A, Scarpa A. Genomic landscape of pancreatic neuroendocrine tumours: the
22 International Cancer Genome Consortium. *J Endocrinol*. 2018;236(3):R161-R7.

23 17. Kahan Yossef Y, Sela Peremen L, Telerman A, Goldinger G, Malitsky S, Itkin M, et al.
24 Single-cell transcriptomics and metabolomic analysis reveal adenosine-derived metabolites over-
25 representation in pseudohypoxic neuroendocrine tumours. *Clin Transl Med*. 2025;15(2):e70159.

26 18. Laks S, van Leeuwaarde R, Patel D, Keutgen XM, Hammel P, Nilubol N, et al.
27 Management recommendations for pancreatic manifestations of von Hippel-Lindau disease.
28 *Cancer*. 2022;128(3):435-46.

29 19. Schmitt AM, Schmid S, Rudolph T, Anlauf M, Prinz C, Kloppel G, et al. VHL
30 inactivation is an important pathway for the development of malignant sporadic pancreatic
31 endocrine tumors. *Endocr Relat Cancer*. 2009;16(4):1219-27.

32 20. Dwight T, Kim E, Bastard K, Benn DE, Eisenhofer G, Richter S, et al. Functional
33 significance of germline EPAS1 variants. *Endocr Relat Cancer*. 2021;28(2):97-109.

34 21. Yang H, Chen Y, Liu K, Zhao L. Case Report: A novel EPAS1 mutation in a case of
35 paraganglioma complicated with polycythemia and atrial septal defect. *Front Endocrinol*
36 (Lausanne). 2023;14:1180091.

37 22. Comino-Mendez I, de Cubas AA, Bernal C, Alvarez-Escola C, Sanchez-Malo C,
38 Ramirez-Tortosa CL, et al. Tumoral EPAS1 (HIF2A) mutations explain sporadic
39 pheochromocytoma and paraganglioma in the absence of erythrocytosis. *Hum Mol Genet*.
40 2013;22(11):2169-76.

41 23. Welander J, Andreasson A, Brauckhoff M, Backdahl M, Larsson C, Gimm O, et al.
42 Frequent EPAS1/HIF2alpha exons 9 and 12 mutations in non-familial pheochromocytoma.
43 *Endocr Relat Cancer*. 2014;21(3):495-504.

44 24. Childebayeva A, Jones TR, Goodrich JM, Leon-Velarde F, Rivera-Chira M, Kiyamu M,
45 et al. LINE-1 and EPAS1 DNA methylation associations with high-altitude exposure.
46 *Epigenetics*. 2019;14(1):1-15.

1 25. Vaidya A, Flores SK, Cheng ZM, Nicolas M, Deng Y, Opotowsky AR, et al. EPAS1
2 Mutations and Paragangliomas in Cyanotic Congenital Heart Disease. *N Engl J Med.*
3 2018;378(13):1259-61.

4 26. Opotowsky AR, Moko LE, Ginns J, Rosenbaum M, Greutmann M, Aboulhosn J, et al.
5 Pheochromocytoma and paraganglioma in cyanotic congenital heart disease. *The Journal of*
6 *clinical endocrinology and metabolism.* 2015;100(4):1325-34.

7 27. Leung AA, Hyrcza MD, Pasieka JL, Kline GA. Incidence of pheochromocytoma and
8 paraganglioma varies according to altitude: meta-regression analysis. *Eur J Endocrinol.*
9 2021;184(5):L21-L3.

10 28. Alzahrani AS, Alswailem M, Buffet A, Alghamdi B, Alobaid L, Alsagheir O, et al.
11 EPAS1-related pheochromocytoma/paraganglioma. *Endocr Relat Cancer.* 2024;31(8).

12 29. Alswailem M, Alghamdi B, Alobaid LA, Al-Hindi H, Aldawish M, Alsagheir O, et al.
13 SAT631 EPAS1 Mutations In Three Adjacent Nucleotides Resulting In Different Phenotypes.
14 *Journal of the Endocrine Society.* 2023;7(Supplement_1).

15 30. Jonasch E, Donskov F, Iliopoulos O, Rathmell WK, Narayan VK, Maughan BL, et al.
16 Belzutifan for Renal Cell Carcinoma in von Hippel-Lindau Disease. *N Engl J Med.*
17 2021;385(22):2036-46.

18 31. Else T, Jonasch E, Iliopoulos O, Beckermann KE, Narayan V, Maughan BL, et al.
19 Belzutifan for von Hippel-Lindau Disease: Pancreatic Lesion Population of the Phase 2
20 LITESPARK-004 Study. *Clin Cancer Res.* 2024;30(9):1750-7.

21 32. Choueiri TK, Bauer TM, Papadopoulos KP, Plimack ER, Merchan JR, McDermott DF, et
22 al. Author Correction: Inhibition of hypoxia-inducible factor-2alpha in renal cell carcinoma with
23 belzutifan: a phase 1 trial and biomarker analysis. *Nat Med.* 2021;27(10):1849.

24 33. Choueiri TK, Powles T, Peltola K, de Velasco G, Burotto M, Suarez C, et al. Belzutifan
25 versus Everolimus for Advanced Renal-Cell Carcinoma. *N Engl J Med.* 2024;391(8):710-21.

26 34. Kamihara J, Hamilton KV, Pollard JA, Clinton CM, Madden JA, Lin J, et al. Belzutifan,
27 a Potent HIF2alpha Inhibitor, in the Pacak-Zhuang Syndrome. *N Engl J Med.*
28 2021;385(22):2059-65.

29 35. Alkaissi H, Talvacchio S, Derkyi A, Gubbi S, Pappo A, Gordon C, et al. Belzutifan for
30 HIF2A-Related Pheochromocytoma and Paraganglioma: A Retrospective Study of Real-World
31 Data. *Endocr Pract.* 2025.

32 36. Alkaissi H, Nazari MA, Hadrava Vanova K, Uher O, Gordon CM, Talvacchio S, et al.
33 Rapid Cardiovascular Response to Belzutifan in HIF2A-Mediated Paraganglioma. *N Engl J*
34 *Med.* 2024;391(16):1552-5.

35 37. Jimenez C, Andreassen M, Durand A, Moog S, Hendifar A, Welin S, et al. Belzutifan for
36 Advanced Pheochromocytoma or Paraganglioma. *N Engl J Med.* 2025.

37 38. Rosenblum JS, Cole Y, Dang D, Lookian PP, Alkaissi H, Patel M, et al. Head and neck
38 paraganglioma in Pacak-Zhuang syndrome. *JNCI Cancer Spectr.* 2025;9(1).

39 39. Blansfield JA, Choyke L, Morita SY, Choyke PL, Pingpank JF, Alexander HR, et al.
40 Clinical, genetic and radiographic analysis of 108 patients with von Hippel-Lindau disease
41 (VHL) manifested by pancreatic neuroendocrine neoplasms (PNETs). *Surgery.* 2007;142(6):814-
42 8; discussion 8 e1-2.

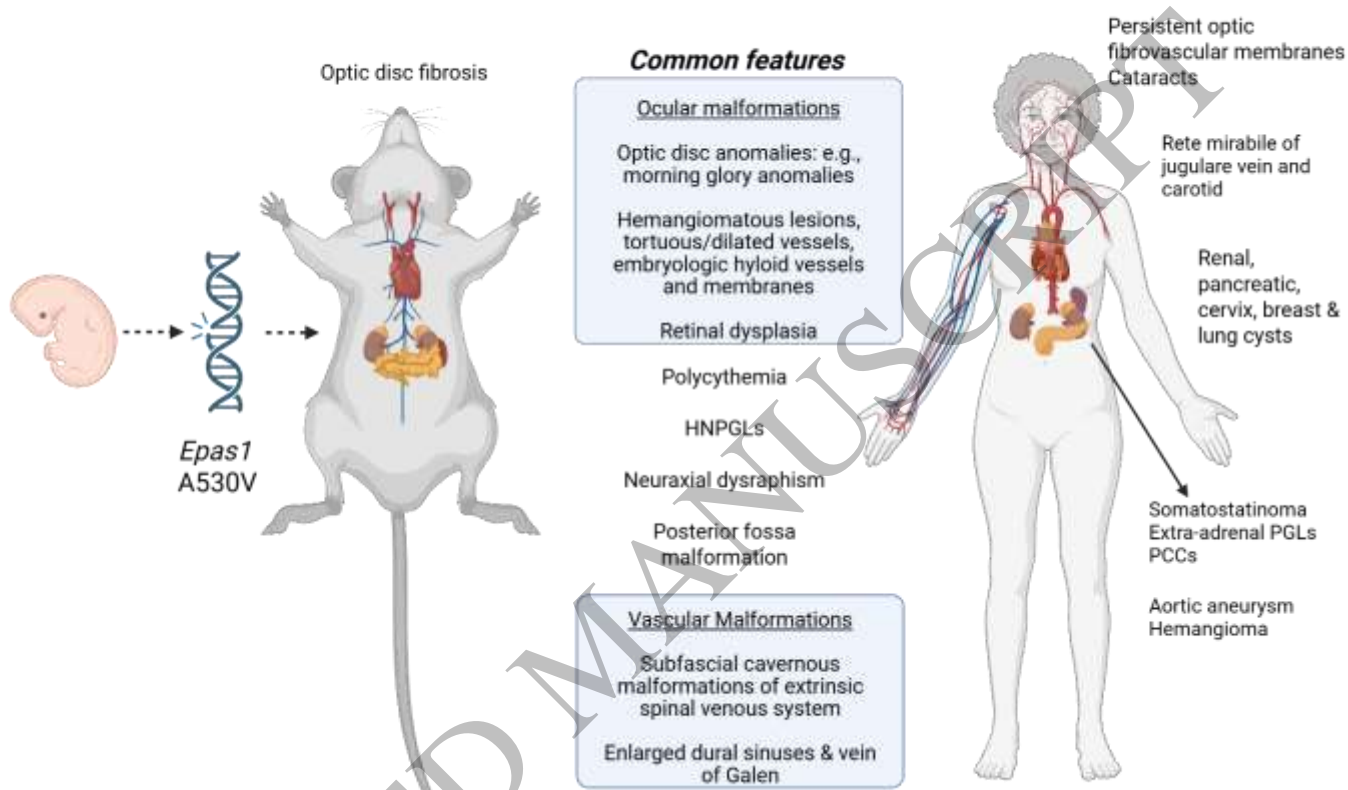
43 40. Chevalier B, Dupuis H, Jannin A, Lemaitre M, Do Cao C, Cardot-Bauters C, et al.
44 Phakomatoses and Endocrine Gland Tumors: Noteworthy and (Not so) Rare Associations. *Front*
45 *Endocrinol (Lausanne).* 2021;12:678869.

1 41. Tanaka A, Ogawa M, Zhou Y, Otani Y, Hendrickson RC, Miele MM, et al.
2 Proteogenomic characterization of pancreatic neuroendocrine tumors uncovers hypoxia and
3 immune signatures in clinically aggressive subtypes. *iScience*. 2024;27(8):110544.
4 42. Zhang Q, Lou Y, Zhang J, Fu Q, Wei T, Sun X, et al. Hypoxia-inducible factor-2alpha
5 promotes tumor progression and has crosstalk with Wnt/beta-catenin signaling in pancreatic
6 cancer. *Mol Cancer*. 2017;16(1):119.
7

8 Figures & Tables

1

Transgenic Mouse Model of Pacak-Zhuang Syndrome



2

3 **Figure 1.** Summary of *EPAS1* associated phenotypes in Pacak-Zhuang syndrome (PZS) and
4 a transgenic murine model. Disease entities were compiled from previously reported
5 publications[6, 9-11, 38]. Phenotypes identified thus far in the *Epas1* murine model and in
6 PZS patients are listed on the left- and right-hand sides respectively, while the middle
7 section lists common phenotypes. Created in BioRender. Cole, Y. (2025)
8 <https://biorender.com/g1a8rco>

9
10

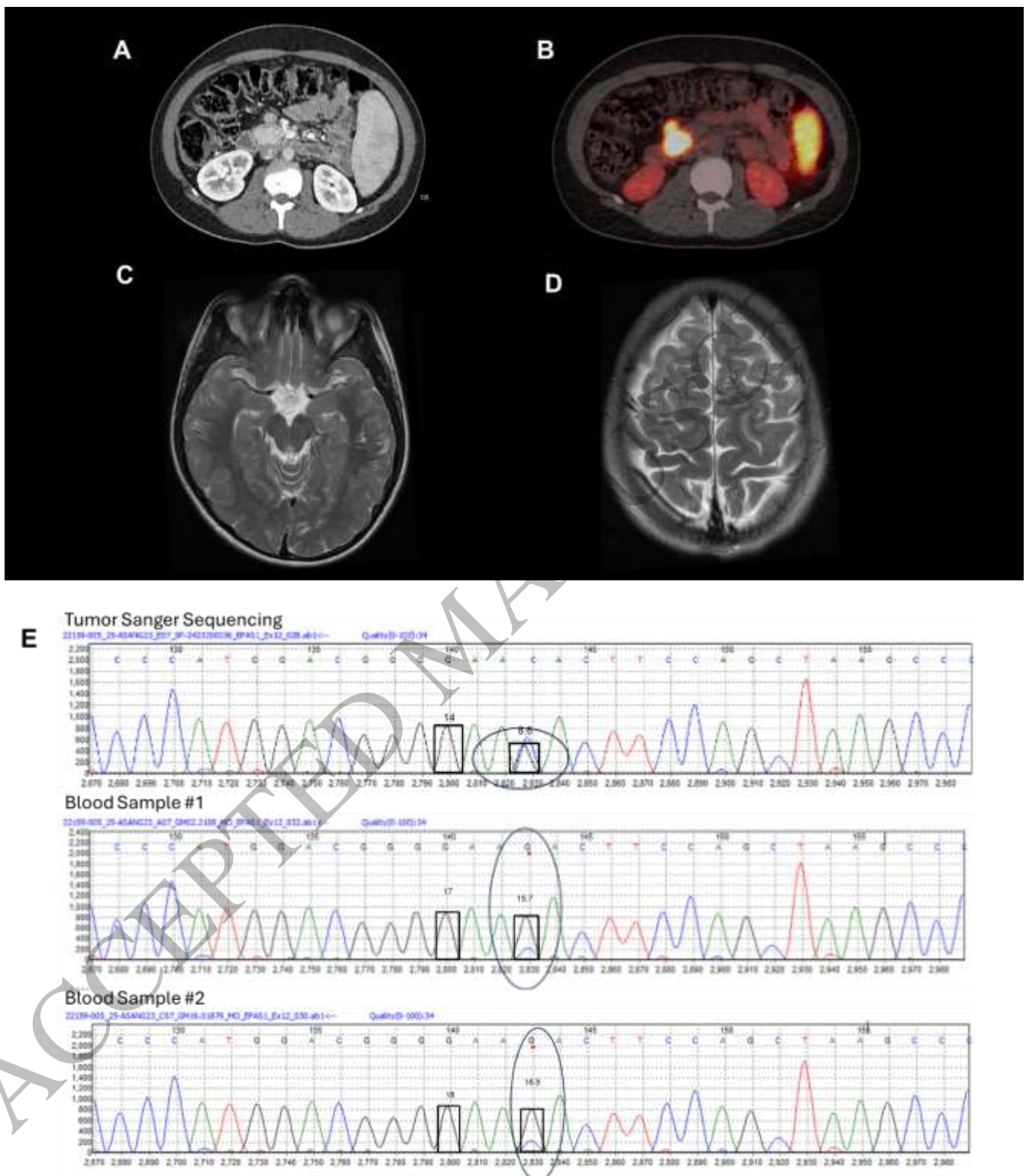
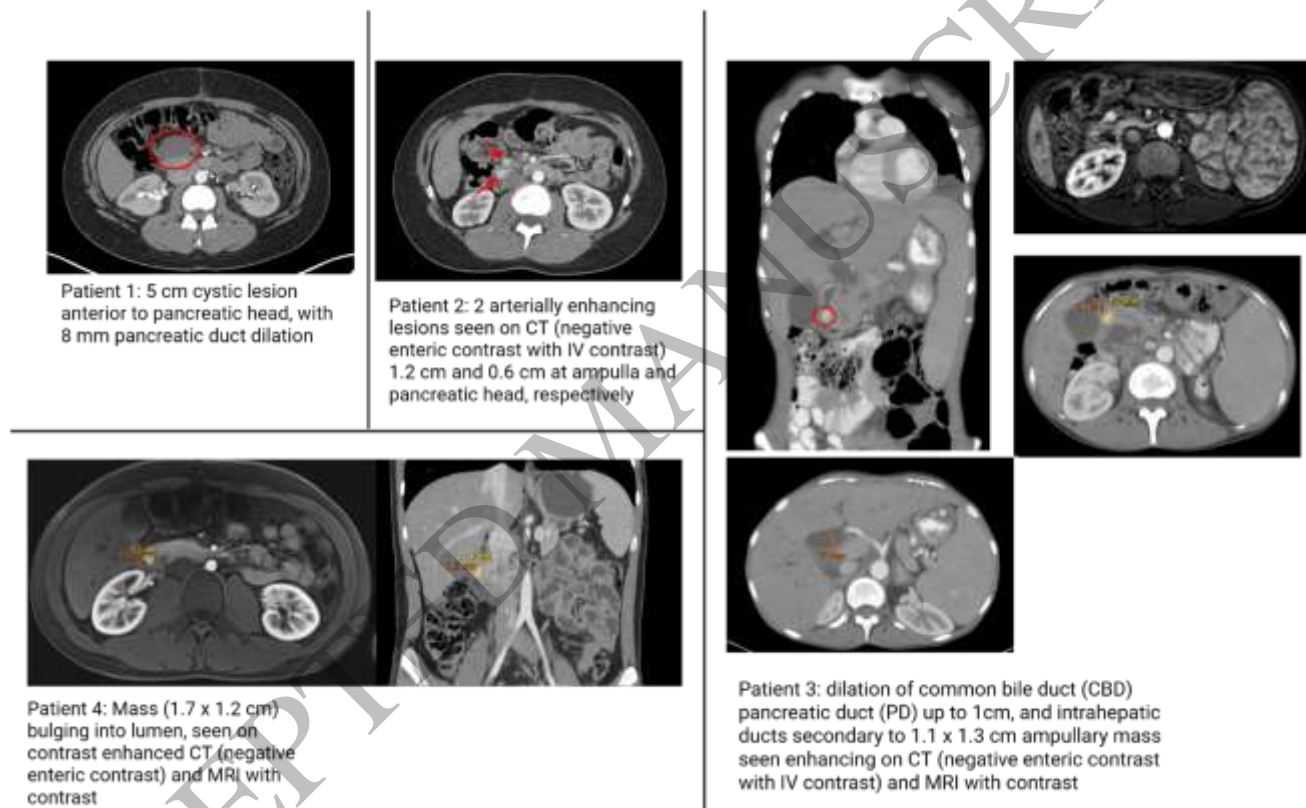


Figure 2. *HIF2A*-Associated Nonfunctional Pancreatic Neuroendocrine Tumor. A: An axial contrast enhanced CT image of the abdomen and pelvis demonstrating a 30mm pancreatic neuroendocrine tumor in the uncinate process and adjacent 10 mm lymph node. B: A

1 sagittal fused image from a $[^{68}\text{Ga}]$ -DOTATATE PET-CT illustrating avidity in the pancreatic
 2 mass and adjacent node. Axial T2-weighted imaging of the brain shows multiple visible and
 3 prominent perivascular spaces in (C) the bilateral subcortical white matter of the temporal
 4 lobes and (D) the bilateral subcortical white matter of the frontal lobes. (E) *EPAS1* variant
 5 allele frequency in both germline (sample #1 15.2%, sample #2 15.4%) and somatic tissue
 6 (pancreatic neuroendocrine tumor) (42.8%) in index case. Created in BioRender. Cole, Y.
 7 (2025) <https://BioRender.com/z607ez6>

8



9

10 **Figure 3.** Somatostatinoma imaging in a Pacak-Zhuang syndrome cohort. CT images are
 11 provided for four individuals with somatostatinomas. Masses are denoted with either a
 12 circle or arrows along with measurements. Only a post-surgical contrast enhanced CT
 13 imaging is available for patient 1 is available and illustrates a post-surgical cyst with
 14 pancreatic duct dilation. Patients 2 and 3 also demonstrate pancreatic duct dilation in
 15 addition to a somatostatinoma. Note: Patient 5 underwent imaging and surgical resection
 16 at an outside institution prior to referral; although the imaging was not available for review,
 17 pathology confirmed the diagnosis of somatostatinoma. Created in BioRender. Cole, Y.
 18 (2025) <https://BioRender.com/9qqp24l>

19

Pacak-Zhuang Syndrome Patient Characteristics

	Patient 1	Patient 2	Patient 3	Patient 4	Patient 5
Age at Initial Diagnosis	Erythrocytosis at age 2	Erythrocytosis at birth	Erythrocytosis at birth	Erythrocytosis at age 2	Erythrocytosis at age 7
Sex	F	F	F	M	F
PPGL (age at first diagnosis)	39	18	14	15	36
PNET (Somatostatinoma)					
Age of Initial Diagnosis (years)	39	23	29	21	36
Multiple somatostatinomas ?	N	Y	Y	Y	Y
Somatostatin (< 25 pg/mL)	31 40	50 (possible recurrence with somatostatin elevated to 30)	109 32	12 NA	36 NA
Age of Recurrence					
Age of Metastatic Disease	39	NA	32	NA	36
Pathological Grade (ki67 index)	NA [#] (2%)	NA [#] (2%\$)	NA [#] (NA [#])	G1 (<3%),	NA [#] (NA [#]),

				somatostatin positive on IHC, invading mucosa, submucosa, and muscularis propria	somatostatin positive on IHC, invading mucosa, submucosa, and muscularis propria
<hr/>					
Catecholamines (plasma)					
Norepinephrine (80-498 pg/mL)	1875	1760	10951	257	775
Epinephrine (4-83 pg/mL)	24	7	100	<20	<20
Dopamine (3-46 pg/mL)	<25	20	28	<25	1091
Normetanephrine (18-112 pg/mL)	1993	858	4834	158	515
Metanephrine (12-61 pg/mL)	77	9	121	<12	<12
<hr/>					
Variant analysis					
<i>EPAS1</i>	p.D539N	p.A530V	p.A530T	p.P531S	p.Y532C
Variant allele frequency (%):					
Blood	Undetect ed	0.80%	12.70%	Undetect ed	Undetect ed
Nail	Undetect ed	Undetected	27.00%	NA	Undetect ed

Hair	Undetect ed	1.80%	12%	Undetect ed	1%
	3.80%	1.30%	17.80%	NA	Undetect ed
	NA*	31% and 37% (two pancreatic lesions)	56%	40%	NA
GI Symptoms	Early satiety, occasional nausea	Episodes of dull epigastric pain without clear triggers or relieving factors	Obstructive jaundice, chronic abdominal pain and nausea/vomiting	None; identified incidentally	Obstructive jaundice
Other Phenotypes	EPO-dependent erythrocytosis, optic disc fibrosis, peripapillary fibrosis, peripapillary tortuosity, with dilated veins, peripapillary gliosis and optic disc drusen in left eye, strabismus with	EPO-dependent erythrocytosis, optic disc fibrosis, vascular fibrosis, tortuosity, with dilated veins, peripapillary gliosis and optic disc drusen in left eye, abnormal retinal vasculature	EPO-dependent erythrocytosis, optic disc fibrosis, peripapillary gliosis and anomalies of both eyes, exotropia of left eye, hemangioblastoma-like lesion in left	EPO-dependent erythrocytosis, optic disc fibrosis, peripapillary gliosis and anomalies of both eyes, exotropia of left eye, hemangioblastoma-like lesion in left	EPO-dependent erythrocytosis, mild optic nerve fibrosis, bilateral cataract (posterior subcapsular), macular oedema and disc fibrosis, HNPGs, lung and

amblyopia and esotropia of left eye, pancreatic cysts, liver lesion on MRI	with tortuous thickened veins and peripheral retinal pigment epithelial changes, bilateral renal cysts, breast cysts	eye, Marfanoid habitus, ascending aortic aneurysm	primarily in R eye	cervical cysts
----------------------------------------------------------------------------	----------------------------------------------------------------------------------------------------------------------	---------------------------------------------------	--------------------	----------------

1
2 **Table 1.** Clinical phenotypes in Pacak-Zhuang syndrome (PZS). Clinical phenotypes and
3 laboratory investigations are provided for four individuals with pancreatic neuroendocrine
4 tumors (somatostatinomas) from a cohort of PZS patients at the NIH. Other phenotypes
5 have been previously published[6]. Age of onset is provided for each phenotype. For
6 somatostatinomas, information regarding disease recurrence is provided. M: molar; μ L:
7 microliter; mIU/mL: milli-international units per milliliter; pg/mL: picograms per milliliter;
8 μ M: micromolar. *Denotes that a variant allele frequency was not available on the tumor
9 #Denotes information was not available/reported in histologic report \$Ki67 index from one
10 of the tumors resected.